Brief Report

DOI: 10.5582/ddt.2011.v5.2.61

Design, synthesis and activity study of aminopeptidase N targeted 3-amino-2-hydroxy-4-phenyl-butanoic acid derivatives

Laizhong Chen, Jiajia Mou, Yingying Xu, Hao Fang, Wenfang Xu*

Department of Medicinal Chemistry, School of Pharmacy, Shandong University, Ji'nan, Shandong, China.

ABSTRACT: A series of (2RS,3S)-3-amino-2-hydroxy-4-phenyl-butanoic acids (AHPA) derivatives (MA0-MA7) were synthesized. The *in vitro* aminopeptidase N (APN) enzyme and cell proliferation assay of target compounds were investigated. The results showed that most compounds displayed potent inhibitory activities against APN, compound MA0 showed even better inhibitory effects than bestatin on both enzyme activity and HL60 cell proliferation. The FlexX docking result showed the mode of binding between MA0 and APN.

Keywords: AHPA derivatives, synthesis, inhibitors, aminopeptidase N

1. Introduction

Aminopeptidase N (APN, EC 3.4.11.2), a zinc-containing metalloprotease removes amino acids sequentially from the N-terminals of peptides and proteins (*1*). APN is widely distributed in the body of mammals, and can be expressed on the surface of various types of cells (*2*). APN was shown to be involved in the degradation of extracellular matrix in tumor invasion. It may serve as a target receptor for drug delivery into tumors and also contribute to angiogenesis (*3*,*4*).

A number of APN inhibitors are known in the literature, but only a few relatively simple compounds have been designed as inhibitors, bestatin [(2S,3R)-3-amino-2-hydroxy-4-phenyl-butanoyl]-L-leucine is one of them (*5*). Bestatin is a slow-binding competitive inhibitor of APN (*6*). The schematic representation of bestatin within the active site of APN is depicted in Figure 1 (*7*). The aromatic ring and the aliphatic chain of the leucine residue can interact with the hydrophobic areas of aminopeptidases (S_1 and S_1'), the amino group can form a hydrogen bond or ionic bond with the residues of the active site, the 2-hydroxyl and the amide carboxyl group can coordinate with metal ions or bind to residues of the active site *via* hydrogen bonds. The S_2' pocket of APN is hydrophobic and vacant because the −COOH of bestatin shortness and hydrophilic character.

Bestatin is a potent inhibitor of APN but is mainly used as an immunopotentiator in clinical settings. It must have greater activity in order for bestatin derivatives to be used directly as an APN inhibitor in clinical settings. Furthermore, many adverse effects of bestatin have been noted, so optimization of bestatin and identification of better inhibitors is an important job. We designed a series of bestatin analogues, which *i*) reserved the most important scaffold (AHPA); *ii*) replaced the −COOH with −COOMe to enhance the interaction between inhibitors and the S_2' pocket of APN; and *iii*) changed the configuration of the chiral centers of AHPA to study the structure-activity relationship.

2. Materials and Methods

2.1. *Chemicals*

The synthetic route is outlined in Scheme 1. Protection of optically pure L-Phe with di-tert-butyl dicarbonate gave compound **1**, which was conveniently converted to compound **2** *via* a condensation reaction with *N*-methoxymethanamine. Hydrogenation of **2** with $LiAlH_4$ gave compound **3**. Reaction of **3** with $NaHSO_3$ and then NaCN gave compound **4**. **4** was hydrolyzed with 6 mol/L HCl and then protected with di-tert-butyl dicarbonate which gave the key intermediate compound

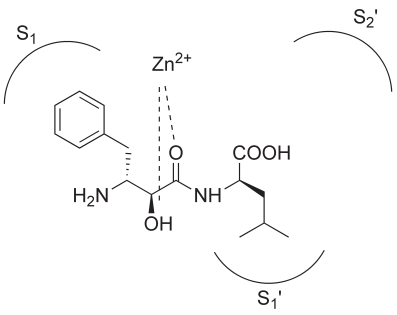

Figure 1. The binding mode of bestatin to the active site of APN.

**Address correspondence to:*
Dr. Wenfang Xu, Department of Medicinal Chemistry, School of Pharmacy, Shandong University, 44 Wenhuaxi Road, Ji'nan 250012, Shandong, China.
e-mail: xuwenf@sdu.edu.cn

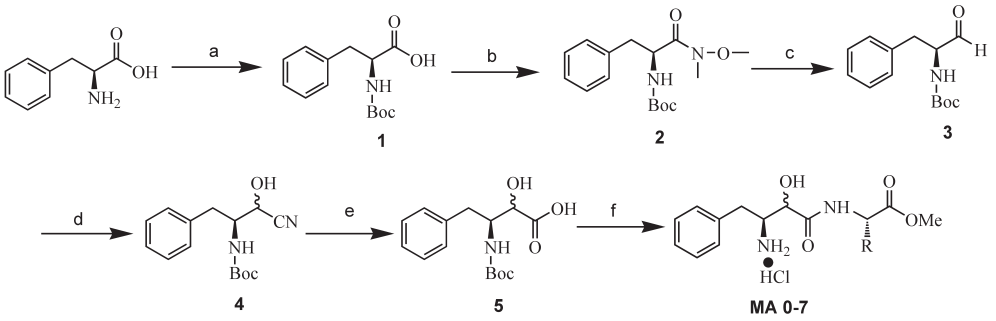

Scheme 1. Reagents and conditions: (a) $(Boc)_2O$, 1 mol/L NaOH, THF; **(b)** TBTU, *N*-methoxymethanamine, TEA, anhydrous DCM; **(c)** $LiAlH_4$, anhydrous THF; (**d**) (*i*) $NaHSO_3$, EtOAc, H_2O; (*ii*) NaCN; **(e)** (*i*) 6 mol/L HCl; (*ii*) $(Boc)_2O$, 1 mol/L NaOH, THF; **(f)** (*i*) HOBt, DCC, TEA, R-COOMe-HCl; (*ii*) 3 mol/L HCl-EtOAc.

5. Reaction of **5** with corresponding the amino acid methyl ester hydrochloride and then 3 mol/L HCl in EtOAc gave compound **MA0-MA7**.

2.2. *APN inhibition assay*

IC_{50} values against APN were determined using L-Leu-*p*-nitroanilide as the substrate and microsomal aminopeptidase (Sigma-Aldrich) as the enzyme in 50 mM PBS, pH 7.2, at 37°C (*8*). The hydrolysis of the substrate was monitored by following the changes in absorbance measured at 405 nm. All solutions of the inhibitors were prepared in the assay buffer, and the pH was adjusted to 7.5 by the addition of 0.1 M HCl or 0.1 M NaOH. All inhibitors were preincubated with APN for 30 min at 37°C. The assay mixture, which contained the inhibitor solution (with its concentration depending on the inhibitor), the enzyme solution (4 μg/mL final concentration), and the assay buffer, was adjusted to 200 μL.

2.3. *Cell proliferation assay*

HL60 cells (with high APN expression) and MDA-MB-231 cells (with low APN expression) were grown in RPMI1640 medium containing 10% FBS at 37°C in a 5% CO_2 humidified incubator. Cell proliferation was determined by the MTT (3-[4,5-dimethyl-2-thiazolyl]-2,5-diphenyl-2H-tetrazolium bromide) assay (*9*). Briefly, cells were plated in a 96-well plate at 1×10^4 cells per well, cultured for 4 h in complete growth medium, then treated with 2,000, 1,000, 500, 250, or 125 μg/mL of compounds for 48 h. 0.5% MTT solution was added to each well. After further incubation for 4h, formazan formed from MTT was extracted by adding DMSO and mixing for 15 min. Optical density was read with an ELISA reader at 570 nm.

2.4. *Docking study*

The docking studies were performed using the FlexX2 docking program in Sybyl7.0 (Tripos Inc., St. Louis, MO, USA) software running on a DELL Precision 390 workstation (*10*). The molecular structures were built based on the conformation of bestatin.

Table 1. The APN inhibitory activities of the target compounds

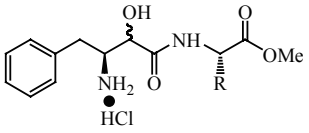

Compound	R	IC_{50} (μmol/L)
MA0		0.17
MA1		4.4
MA2		13
MA3		18
MA4	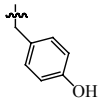	5.9
MA5		> 1000
MA6		3.8
MA7	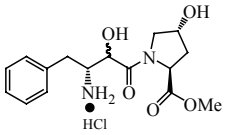	163
bestatin		0.34

Energy minimization was performed using Powell optimization in the presence of the Tripos force field with a convergence criterion of 0.05 kcal/mol•Å and then assigned with the Gasteiger-Hückel charges. In the docking process, maximum number of poses per ligand was set to 30 and other parameters were set as default.

3. Results and Discussion

All inhibition results are shown in Table 1 and Table 2. The FlexX docking results of bestatin and compound

Table 2. The cell growth inhibition activities of MA0 and bestatin

Compound	IC_{50} of HL60 cell (μmol/L)	IC_{50} of MDA-MB-231 cell (μmol/L)
MA0	20.8	204
bestatin	31.4	85.7

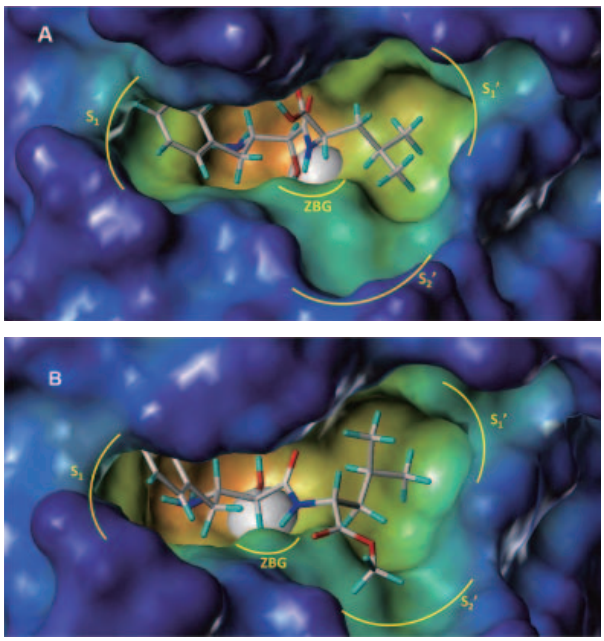

Figure 2. (A) The FlexX Docking of bestatin with APN; (B) The FlexX Docking of MA0 with APN.

MA0 with APN are shown in Figures 2A and 2B. Compound **MA0** showed stronger activity than bestatin which indicates that protection of the carboxyl group of bestatin with methyl ester can improve its activity. Because the S_2' pocket of APN is vacant in the binding mode of bestatin to APN, the enhanced activity of **MA0** may be due to the −COOMe that can form a hydrophobic interaction with the S_2' pocket of APN, as shown in the FlexX docking result (Figure 2B).

MA0 showed stronger activity than bestatin despite that its configuration is different from bestatin which indicates that the configuration of AHPA is not very strict when binding to APN. As shown in the FlexX docking result (Figures 2A and 2B), both (2S, 3R)-AHPA and (2RS, 3S)-AHPA can interact with the active site tightly.

All the target componds showed potent activities to APN except **MA5**, which indicates that the side chains of the amino acid residues are important because they can form hydrophobic interactions with the S_1' pocket of APN. **MA1** showed stronger activity than **MA4**, which may be due to the phenyl group which is more hydrophobic than the phenolic group. The activity of **MA2** is weaker than **MA0**, which suggests that the length of the side chain is important for enzyme inhibition.

4. Conclusion

In conclusion, eight AHPA derivatives were synthesized as APN inhibitors. Most of the compounds showed potent activity against APN, **MA0** not only exhibited stronger enzymatic inhibition compared with the natural APN inhibitor bestatin, but also showed better cell growth inhibition activity on HL60 cells with high expression of APN. The structure-activity relationship indicates that enhancing the interaction between bestatin derivatives and S_2' is useful in further optimization of bestatin.

Acknowledgements

The work was supported by National Natural Science Foundation of China (No. 30772654), Major Program of the National Natural Science Foundation of China (No. 90713041), National High Technology Research and Development Program of China (863 Program) (No. 2007AA02Z314).

References

1 Bauvois B, Dauzonne D. Aminopeptidase-N/CD13 (EC 3.4.11.2) inhibitors: Chemistry, biological evaluations, and therapeutic prospects. Med Res Rev. 2006; 26:88-130.
2 Zhang X, Xu W. Aminopeptidase N (APN/CD13) as a target for anti-cancer agent design. Curr Med Chem. 2008; 15:2850-2865.
3 Saiki I, Yoneda J, Azuma I, Fujii H, Abe F, Nakajima M, Tsuruo T. Role of aminopeptidase N (CD13) in tumor-cell invasion and extracellular matrix degradation. Int J Cancer. 1993; 54:137-143.
4 Inagaki Y, Tang W, Zhang L, Du GH, Xu WF, Kokudo N. Novel aminopeptidase N (APN/CD13) inhibitor 24F can suppress invasion of hepatocellular carcinoma cells as well as angiogenesis. BioSci Trends. 2010; 4:56-60.
5 Gordon EM, Godfrey JD, Delaney NG, Asaad M M, Von Langen D, Cushman DW. Design of novel inhibitors of aminopeptidases. Synthesis of peptide-derived diamino thiols and sulfur replacement analogs of bestatin. J Med Chem. 1988; 31:2199-2211.
6 Mishima Y, Terui Y, Sugimura N, Matsumoto-Mishima Y, Rokudai A, Kuniyoshi R, Hatake K. Continuous treatment of bestatin induces anti-angiogenic property in endothelial cells. Cancer Sci. 2007; 98:364-372.
7 Yang K, Wang Q, Su L, Fang H, Wang X, Gong J, Wang B, Xu W. Design and synthesis of novel chloramphenicol amine derivatives as potent aminopeptidase N (APN/CD13) inhibitors. Bioorg Med Chem. 2009; 17:3810-3817.
8 Zhang J, Li X, Zhu HW, Wang Q, Feng JH, Mou JJ, Li YG, Fang H, Xu WF. Design, synthesis, and primary activity evaluation of pyrrolidine derivatives as matrix metalloproteinase inhibitors. Drug Discov Ther. 2010; 4:5-12.
9 Zhang X, Fang H, Zhu H, Wang X, Zhang L, Li M, Li Q, Yuan Y, Xu W. Novel aminopeptidase N (APN/CD13) inhibitors derived from 3-phenylalanyl-N'-substituted-

2,6-piperidinedione. Bioorg Med Chem. 2010; 18:5981-5987.
10 Zhang L, Fang H, Zhu HW, Wang Q, Xu WF. QSAR studies of histone deacetylase (HDAC) inhibitors by CoMFA, CoMSIA, and molecular docking. Drug Discov Ther. 2009; 3:41-48.

(Received December 09, 2010; Revised December 29, 2010; Accepted January 24, 2011)

Appendix

1. Chemistry: general procedures

All materials were purchased from commercial suppliers and used without further purification. Solvents were distilled prior to use and all the reactions were monitored by thin-layer chromatography on 0.25 mm silica gel plates (60GF-254) and visualized with UV light or ninhydrin. Proton nuclear magnetic resonance (^{1}H-NMR) spectra were recorded at 300 MHz. Chemical shifts are reported in delta (δ) units, parts per million (ppm) downfield from trimethylsilane. ESI-MS were determined on an API 4000 spectrometer. Melting points were determined on an electrothermal melting point apparatus (uncorrected).

1.1. (S)-2-(tert-butoxycarbonyl)-3-phenylpropanoic acid (1)

To a stirred solution of L-phe (24.7 g, 150 mmol) in 1 N NaOH (170 mL) at 0℃ was added dropwise to the solution of $(Boc)_2O$ (32.7 g, 165 mmol) in THF (100 mL). The stirring was continued for 1 h at 0° C and then for 10 h at room temperature. The pH of the mixture was maintained at 9-10 during the whole process. The mixture was concentrated and then washed with petroleum ether (100 mL × 3). After the aqueous phase was adjusted to pH 2 with 1 N $KHSO_4$, a white precipitation appeared. The mixture was filtered to afford compound **1** (37.8 g), yield 95%, m.p. 83-85°C.

1.2. (S)-tert-butyl 1-(methoxy(methyl)amino)-1-oxo-3-phenylpropan-2-ylcarbamate (2)

To a stirred solution of compound **1** (2.65 g, 10 mmol), Et_3N (3.6 mL, 25 mmol) at rt. in CH_2Cl_2 (30 mL) was added TBTU (4.8 g, 15 mmol). The mixture was stirred for 15 min, and *N,O*-dimethylhydroxylamine hydrochloride (1.07 g, 0.11 mmol) was added. The mixture was stirred for 12 h until reaction completion (checked by TLC in PE/EtOAc 2:1). The reaction mixture was washed sequentially with 10% citric acid (30 mL × 3), saturated $NaHCO_3$ (30 mL × 2), and finally with brine. The organic layer was dried over Na_2SO_4 and evaporated to give a colorless oil (2.94 g, 95.5%).

1.3. (S)-tert-butyl 1-oxo-3-phenylpropan-2-ylcarbamate (3)

Compound **2** (2.94 g, 9.5 mmol) was dissolved in anhydrous THF (20 mL) and $LiAlH_4$ (0.53 g, 14 mmol) was slowly added at −20℃. After stirring for 30 min at the same temperature, the mixture was adjusted to pH 7 with 1 N $NaHSO_4$. After filtration, the filtrate was concentrated with a rotary evaporator. The residue was dissolved in EtOAc and washed with 1 N HCl and brine. The EtOAc solution was dried over Na_2SO_4 and concentrated with a rotary evaporator to afford crude product (2.16 g, 91%), which was used without further purification.

1.4. (S)-tert-butyl 1-cyano-1-hydroxy-3-phenylpropan-2-ylcarbamate (4)

To a solution of compound **3** (1.08 g, 4.3 mmol) in EtOAc (20 mL), $NaHSO_3$ (0.69 g, 6.4 mmol) in H_2O (20 mL) was added at 0℃. The mixture was stirred for 5 h at 0℃, NaCN (0.316 g, 6.4 mmol) was added at 0℃, and the stirring was continued for 10 min at 0℃ and then 7 h at room temperature. The EtOAc phase was washed with H_2O and then evaporated to leave the cyanohydrin as an oil. The oil was recrystallized using EtOAc/*n*-hexane (1/5) to afford a white solid (0.82 g, 68.7%).

1.5 (S)-tert-butyl 1,1-dihydroxy-3-phenylpropan-2-ylcarbamate (5)

Compound **4** (0.82 g, 3 mmol) was dissolved in 6 N HCl (20 mL), and the solution was gently refluxed and stirred for 7 h. The hydrolysis reaction was allowed to cool and then concentrated in vacuo to give a brown oil. The residue was dissolved in water (50 mL) and pH adjusted to 10 with 3 N NaOH. The solution of $(Boc)_2O$ (0.78 g, 3.6 mmol) in THF (50 mL) was added dropwise to the mixture at 0℃. The reaction was stirred for 1 h at 0℃ and then 10 h at room temperature, while the pH was maintained at pH 11 with 1 N NaOH. The mixture was concentrated and then washed with petroleum ether (50 mL × 3). The aqueous phase was adjusted to pH 2 with 1 N $KHSO_4$, and extracted with EtOAc (20 mL × 3). The organic phase was dried with $MgSO_4$ and concentrated in vacuo to yield a white solid 0.56 g, 63.2%. ^{1}H-NMR (300 MHz, DMSO-d6) δ: 7.24 (m, 5H), 6.39 (d, 1H, J = 9.6 Hz), 3.97 (d, 1H, J = 9.0), 3.84 (m, 1H), 2.79 (dd, 1H, J = 13.2, 7.2), 2.67 (dd, 1H, J = 12.6, 7.2), 1.29 (s, 9H).

1.6. (S)-methyl 2-((S)-3-amino-2-hydroxy-4-phenylbutanamido)-4-methylpentanoate (MA0)

Compound **5** (2.15 g, 8 mmol) was dissolved in anhydrous THF (70 mL), HOBt (1.08 g, 8 mmol) and was added to the stirred solution. After 5 min,

the solution of DCC (1.80 g, 8.8 mmol) in anhydrous THF (150 mL) was added to the mixture at 0℃. The mixture was stirred for 0.5 h at 0℃ and then 4 h at room temperature. The mixture was filtered, L-Leucine methyl ester hydrochloride (1.45 g, 8 mmol) and Et_3N (1.15 mL, 8 mmol) was added to the filtrate. The mixture was stirred for 10 h at room temperature and concentrated and then redissolved in EtOAc (50 mL). The solution was washed with 10% citric acid (30 mL × 3), saturated $NaHCO_3$ (30 mL × 2), and finally with brine. The organic layer was dried over Na_2SO_4 and evaporated to give a white solid. The white solid in 20 mL EtOAc saturated with HCl gas was stirred at room temperature for 2 h. The mixture was filtered to obtain the target compound **MA0** (1.4 g). Yield 79.0%, ESI-MS $[M + 1]^+$, m/z: 323.1. ^{1}H-NMR (300 MHz, CD_3OD): 7.36 (m, 5H), 4.49 (m, 1H), 4.13 (d, 1H, *J* = 2.7 Hz), 3.85 (m, 1H), 3.78 (s, 3H), 3.14 (dd, 1H, *J* = 13.8, 8.4 Hz), 2.99 (dd, 1H, *J* = 13.8, 6.6 Hz), 1.70 (m, 3H), 0.95 (d, 6H, *J* = 10.8 Hz). Compounds **MA0**-**MA7** were synthesized following the procedure described above.

(S)-methyl 2-((S)-3-amino-2-hydroxy-4-phenylbutanamido)-3-phenylpropanoate (MA1)

White solid, yield 69.2%, ESI-MS $[M + 1]^+$, m/z: 356.6. ^{1}H-NMR (300 MHz, CD_3OD): 7.28 (m, 10H), 4.32 (m, 1H), 4.03 (d, 1H, *J* = 2.7 Hz), 3.78 (s, 3H), 3.69 (m, 1H), 3.24 (dd, 1H, *J* = 14.1, 5.4 Hz), 3.10 (dd, 1H, *J* = 14.1, 6 Hz), 2.99 (m, 2H).

(S)-methyl 2-((S)-3-amino-2-hydroxy-4-phenylbutanamido)-3-methylbutanoate (MA2)

White solid, yield 68.3%. ESI-MS $[M + 1]^+$, m/z: 281. ^{1}H-NMR (300 MHz, CD_3OD): 7.36 (m, 5H), 4.38 (m, 2H), 3.85 (m, 1H), 3.74 (s, 3H), 3.03 (dd, 1H, *J* = 14.4, 2.4 Hz), 2.90 (dd, 1H, *J* = 14.4, 9.9), 1.42 (d, 3H, *J* = 7.5).

(S)-3-((S)-3-amino-2-hydroxy-4-phenylbutanamido)-4-methoxy-4-oxobutanoic acid (MA3)

White solid, yield 78.4%. ESI-MS $[M + 1]^+$, m/z: 324. ^{1}H-NMR (300 MHz, CD_3OD): 7.35 (m, 5H), 4.52 (q, 1H, *J* = 7.2 Hz), 4.11 (d, 1H, *J* = 4.8 Hz), 3.78 (s, 3H), 3.73 (m, 1H), 3.13 (m, 1H), 2.99 (m, 1H), 1.45 (d, 2H, *J* = 7.2 Hz).

(S)-methyl 2-((S)-3-amino-2-hydroxy-4-phenylbutanamido)-3-(4-hydroxyphenyl)propanoate (MA4)

White solid, yield 85.4%. ESI-MS $[M + 1]^+$, m/z: 372. ^{1}H-NMR (300 MHz, CD_3OD): 7.16 (m, 10H), 4.72 (dd, 1H, *J* = 9.3, 2.1 Hz), 4.37 (d, 1H, *J* = 3.3 Hz), 3.74 (s, 3H), 3.67 (m, 1H), 3.16 (dd, 1H, *J* = 14.1, 5.1 Hz), 2.96 (dd, 1H, *J* = 14.1, 9.1 Hz), 2.66 (dd, 1H, *J* = 14.7, 10.5 Hz) , 2.48 (dd, 1H, *J* = 14.7, 4.2 Hz).

(S)-methyl 2-(3-amino-2-hydroxy-4-phenylbutanamido)acetate (MA5)

White solid, yield 75.6%. ESI-MS $[M + 1]^+$, m/z: 267.3. ^{1}H-NMR (300 MHz, CD_3OD): 7.32 (m, 5H), 4.41 (d, 1H, *J* = 3.3 Hz), 4.00 (d, 1H, *J* = 17.4 Hz), 3.93 (d, 1H, *J* = 17.4 Hz), 3.83 (m, 1H), 3.74 (s, 3H), 3.17 (dd, 1H, *J* = 14.7, 4.8 Hz), 2.90 (dd, 1H, *J* = 14.7, 9.6 Hz).

(S)-methyl 2-((S)-3-amino-2-hydroxy-4-phenylbutanamido)-4-(methylthio)butanoate (MA6)

White solid, yield 65.2%. ESI-MS $[M + 1]^+$, m/z: 341. ^{1}H-NMR (300 MHz, CD_3OD): 7.35 (m, 5H), 4.61(dd, 1H, *J* = 8.7, 5.1 Hz), 4.42 (d, 1H, *J* = 3.3 Hz), 3.8(m, 1H), 3.76 (s, 3H), 3.02 (dd, 1H, *J* = 14.1, 4.8 Hz), 2.91 (dd, 1H, *J* = 14.1, 9.6 Hz), 2.57 (m, 2H), 2.24 (m, 2H), 2.08 (m, 3H).

(2S,4R)-methyl 1-((S)-3-amino-2-hydroxy-4-phenylbutanoyl)-4-hydroxypyrrolidine-2-carboxylate (MA7)

White solid, yield 77.3%. ESI-MS $[M + 1]^+$, m/z: 306.4. ^{1}H-NMR (300 MHz, CD_3OD): 7.39 (m, 5H), 4.61 (t, 1H, *J* = 8.4 Hz), 4.52 (m, 1H), 4.45 (d, 1H, *J* = 3.6 Hz), 4.24 (m, 2H), 3.73 (s, 3H), 3.59 (m, 1H), 3.02 (d, 2H, *J* = 7.8 Hz), 2.35 (m, 1H), 2.08(m, 1H).